

Copper (II) ion removal from synthetic wastewater using chitosan-impregnated coconut shell adsorbent: optimization, kinetic, and thermodynamic studies

O. Oribayo^{1,*}, O. Olamigoke², A. A. Amoo³

^{1,3}Department of Chemical Engineering, University of Lagos, Nigeria

²Department of Petroleum and Gas Engineering, University of Lagos, Nigeria

*Email: ooribayo@unilag.edu.ng

Abstract

A chitosan-impregnated coconut shell adsorbent composite was prepared for copper (II) ions adsorption from synthetic wastewater. Optimization and characterization of the prepared composite adsorbent was conducted along with the kinetics and thermodynamics experiments. Optimization investigation was achieved using Box-Behnken-based response surface methodology. The highest adsorption factors was obtained, yielding a copper removal efficiency of 76.82% at pH of 6, shaking speed of 150 rpm and initial concentration of 150 mg/g. Maximum Cu²⁺ ion adsorption capacity of 53.49 mg/L was obtained. The experimental data for chitosan-impregnated coconut shell adsorbent composite was analyzed using the kinetic and equilibrium adsorption isotherm models. The Langmuir adsorption isotherm model fit the experimental data, which suggests a highly energetic heterogeneous surface, with an R² of 0.9993. Pseudo-second order explicitly represents the kinetic data with R² range of 0.9989 to 0.9998, indicating a strong correlation between the actual and calculated values. In conclusion, the thermodynamic parameters change in Gibbs's free energy (ΔG), change in enthalpy (ΔH), and change in entropy (ΔS) indicates copper ion adsorption onto chitosan-impregnated coconut shell adsorbent composite was endothermic and spontaneous. These results suggest that chitosan-impregnated coconut shell adsorbent composite is an excellent adsorbent for removing copper ions from wastewater.

Keywords: Optimization, Adsorption, Isotherm, kinetics, Environmental protection

1.0 INTRODUCTION

Pollution significantly impacts the environment negatively by contaminating air, water and soil, putting human health and ecosystems at risk. Hence, the environment will continue to deteriorate until solutions are provided to the pollution problem. Improper disposal of coconut shells can lead to significant environmental pollution. When burned, they release harmful pollutants into the air, contributing to respiratory issues and climate change. In landfills, they decompose slowly, producing methane, a potent greenhouse gas. Near water bodies, decomposing shells can cause nutrient runoff, leading to algal blooms (which can also lead to eutrophication) and harm the ecosystems. Water is crucial for sustaining life and maintaining natural processes. Consequently, before being released into the environment, industrial wastewater containing heavy metals must be treated in accordance with regulations set by regulatory bodies (Vaiopoulou and Gikas, 2012).

In recent decades, increment of heavy metals in higher concentration has been reported in marine ecosystems. These metals identified as toxic are being released into water bodies in quantities that pose risk to human health (Abdel-Ghani *et al.*, 2014). This global issue of water pollution from toxic heavy metals due to wastewater release is germane environmental concern (Aydin *et al.*, 2008). When concentrations of heavy metals like copper (Cu), lead (Pb), cadmium (Cd), and zinc (Zn) in water are above specific limits, they become dangerous to people and other living things. The World Health Organization states that 2.1 mg/L is the maximum amount of copper that can be present in drinkable water.

Mining, smelting, electroplating, brass manufacturing and petroleum refining industries, generate substantial amounts of wastewater and sludge with varying concentrations of Cu (II) ions, which can negatively impact aquatic environments. Aquatic habitats may be adversely affected by the large volumes of untreated wastewater and sludge produced by these enterprises, which contain different proportions of Cu (II) ions. Additionally, sea foods, such as shellfish, mushrooms, and crabs may have copper contaminants due to water pollution (Ganji, 2024).

Variety of methods, including chemical, biological, and physical processes are being employed to treat wastewater in eliminating harmful and toxic contaminants. These methods include adsorption, bio-sorption, solvent extraction, chemical precipitation, reverse osmosis, ion exchange, filtering, and membrane techniques (Wang *et al.*, 2009; Oribayo *et al.*, 2020; Bouhamed *et al.*, 2012). Among these, adsorption is a promising approach with activated carbon made from waste materials proving to be very effective, according to Acharya *et al.* (2009), Xue, *et al.* (2016), and Liu *et al.* (2023). Adsorption is a good method for removing heavy metal ions from water, as it is both efficient and cost-effective. Activated carbons are particularly useful owing to their large surface area, well-developed pores and the high production costs have led researchers to explore cheaper, renewable materials for making activated carbon.

Coconut-based carbon activated adsorbent is often preferred for its excellent surface area as well as porosity, providing excellent adsorption properties. It is known for its effectiveness in removing a wide range of contaminants, including heavy metals. In addition, coconut shell-based carbon activated adsorbent is generally cheap in comparison to others. However, the specific cost can vary based on factors such as production scale, source, and processing methods. Chitosan derived from snail shells is commonly used in eliminating heavy metals from wastewater treatment as a result of its unique properties, including amino(-NH₂) and hydroxyl(-OH) functional groups that can complex alongside heavy metal ions. It is known for its biocompatibility and biodegradability.

In recent times, studies have been done because of these distinctive features of coconut-based activated carbon and chitosan. Hafez *et al.* (2002) used carboxyl methyl chitosan-activated carbon derivatives for the adsorption of copper in industrial wastewater. They obtained the highest removal efficiency of 95.9% and the adsorption of the metals onto the synthesized adsorbent obey Langmuir adsorption isotherm, with correlation coefficients R² ranging from 0.999 to 1. Furthermore, the study also shows that sulphuric acid effectively activates the carbon generated from composite materials. Darweesh *et al.* (2022) researched on removing copper from wastewater with banana leaves activated carbon adsorbent. The optimum removal efficiency of copper ion obtained was 48.7%, with R² of 0.9999 and maximum adsorption capacity of 66.2 mg/g. This result indicate that agricultural waste-based banana adsorbent can remove Cu²⁺ ion in wastewater. However, different adsorbate solution pH and interacting effect of adsorption parameters on Cu²⁺ ion removal efficiency was not considered in this study. In addition, Seleman *et al.* (2023) used powdered banana peeled waste to remove copper from textile effluent. Highest removal efficiency of 83 % was attained under optimal conditions at initial concentration of 80 mg/L at pH 6, adsorbent dosage of 2 g, contact time of 90 minutes and adsorption capacity of 2.3 mg/g. However, this shows that powdered banana peeled adsorption capacity is not favourable compared to the novel composite materials of coconut shell AC and chitosan which have higher optimum removal efficiency.

Though highly sought-after scholarly work provides information pertaining to the removal of copper ions in aqueous solution via using adsorbents as precursors, most of these studies involves modifying a single process factor while maintaining all other variables at a constant level. It is known that the adsorption techniques are not a single variable system but multivariable and the aforementioned conventional approach cannot point out the synergistic effect among multiple process variables. Response surface methodology (RSM) circumvents this restriction and has been widely used in numerous fields of research. Herein, composite of chitosan-impregnated coconut shell adsorbent was synthesised and the best operating conditions for the adsorption of Copper ion removal from synthetic wastewater was obtained using RSM. The prepared composite of chitosan-impregnated coconut shell adsorbent presents both practical applications and opportunities. In practice, this adsorbent could be utilized in treating industrial wastewater, especially in industries such as mining and electroplating where copper is a common contaminant (Smith *et al.*, 2020). It also holds promise for municipal water treatment facilities to ensure clean drinking water by eliminating copper contaminants (Johnson & Lee, 2019). In addition, by combining the input factors for the adsorption process (pH, shaking speed and concentration), an equation that depicts the experimental data was generated.

The explicit purpose of our research was (i) to synthesis composite of chitosan-impregnated coconut shell adsorbent using hydrochloric acid as activating agent and evaluate the adsorption characteristics and potential; (ii) enhancing the adsorption process for removing copper ions from acidic solutions using response surface methodology via varying initial concentration (mg/L), shaking speed (rpm) and pH; (iii) assess the relevance of different adsorption isotherm models to identify the most precise model for Cu^{2+} ions adsorption; and (iv) examine the impact of thermodynamics effects on the adsorption study. This research aims to address as well as proffer a lasting solution to both water and solid waste environmental pollution problems simultaneously.

2.0 MATERIALS AND METHOD

2.1 Materials Used

Coconut shell and snail shell was sourced from Oyingbo, Lagos, Nigeria. The coconut shell and snail shell were cleansed with distilled water to eliminate dirt and impurities and then dried in an oven. All chemicals used were of analytical grade, purchased at Shangai Chemical Reagents Co. Ltd., in China. These chemicals included NaOH, HCl, and Copper (II) tetraoxosulphate (VI) (CuSO_4) salt. In addition, deionized water was employed for preparing samples and cleaning glassware.

2.1.1 Preparation of Chitosan

The steps employed in the production of chitosan include Demineralization, Deproteinization, Decolorization and Deacetylation. During the Demineralization stage, 100g of snail shells were soaked in 1L of 1M HCl for 24 hours. After 24 hours, the soaked powder decanted and washed with deionized water until pH 7 was attained. The washed, demineralized snail shell powder was then soaked in 1L of 1M NaOH for 24 hours. After 24 hours, the soaked snail shell powder decanted; cleansed thoroughly with distilled water until a pH 7 attained. The product obtained after getting a neutral pH (pH 7) is called Chitin. The wet Chitin was oven-dried for 6 hours at 105°C. This stage is known as the Deproteinization stage. The dried unbleached chitin was then soaked in hydrogen peroxide for a period of 24 hours for decolorization. The chitin was then decanted and cleansed with deionized water to a pH 7 and dried in oven for

3 hours and at temperature of 105°C. During the Deacetylation stage, 50 g of dried bleached chitin was soaked in 200 ml of 12.5 M NaOH for 24 hours. It was then decanted and washed thoroughly to reach a pH of 7. The product obtained after the aforementioned stages is known as Chitosan. The wet chitosan was subjected to drying in an oven at a temperature of 105°C. The dried Chitosan was subsequently kept in an airtight jar.

2.2.2 Preparation of Chitosan-impregnated Coconut Shell Adsorbent

Pretreated coconut shell (520 g) was transformed into carbon by heating in a furnace at 500°C for 1 hour and subsequently cooled to obtain carbonized material. For chemical activation, (40 g) batches of the carbonized sample were mixed with 900 ml of 1M HCl, using an activation ratio of 2:1, and allowed to react in a beaker for 1 hr. The mixture underwent filtration to produce a viscous slurry and subjected to heating inside the muffle furnace at 700°C for 30 minutes. After activation, the sample was acid-rinsed with distilled water until the pH of the activated carbon approached neutrality (7.0). Finally, the cleaned sample heated in an electric oven at 120°C, pulverized and screened to get the coconut shell activated carbon required for adsorption experiments. To produce the composite chitosan-impregnated coconut shell adsorbent, activated carbon and chitosan were mixed in ratio of 1:2, homogenized and cured through drying at 105°C to achieve a stable material suitable for environmental remediation applications.

2.3 Characterization Methods

The internal framework and surface characteristics of the chitosan-impregnated coconut shell adsorbent were examined using scanning electron microscopy (Quanta 200 FEG, USA). Additionally, Fourier-transform infrared (FTIR) analysis of the chitosan-impregnated activated carbon was conducted with a Nicolet IS10 spectrophotometer by Thermo Scientific USA.

2.4 Experimental Design

RSM was utilized to design experimental runs for optimization studies. This encompasses a collection of statistical methods and math's focused on development, refining, and optimizing processes (Myers et al., 2016). Parameters including pH, shaking speed, and initial concentrations were assessed at three different levels, with their ranges as represented in Table 1.

Table 1: Box-Behnken Design Implemented in Design expert

Factor	Notation	Units	Low	High	Coded	values
pH	A		3.00	9.00	-1.00	1.00
Concentration	B	(mg/L)	50.00	150.00	-1.00	1.00
Shaking Speed	C	(rpm)	100.00	150.00	-1.00	1.00

By applying the Box-Behnken design, Cu (II) ions removal efficiencies were obtained using seventeen experimental runs. A second-order polynomial equation (Equation 16) was used to analyze the most significant impacts and interactions among the process variables. Analysis of Variance on the experimental data was used to evaluate the model's and these variables' relevance. If the probability value of a variable or interaction is less than the designated

significance level ($P < 0.05$), it is considered significant. Likewise, the model is deemed adequate for process prediction if the P value is below 5%. The summarized results of copper removal efficiency in wastewater are presented in the Table 2 below.

Table 2: Results showing actual and predicted removal efficiency of copper

Run	pH	Concentration (mg/L)	Shaking speed (rpm)	Actual removal efficiency of Cu (%)	Predicted removal efficiency of Cu (%)
1	6	100	125	67.56	67.86
2	9	150	125	63.71	63.73
3	6	100	125	67.72	67.86
4	6	100	125	68.02	67.86
5	9	100	100	59.13	58.90
6	6	150	150	76.82	76.58
7	3	100	100	67.67	67.45
8	6	100	125	68.07	67.86
9	3	100	150	69.76	69.99
10	6	50	100	64.38	64.62
11	6	50	150	66.01	65.80
12	3	150	125	71.23	71.24
13	9	50	125	57.88	57.87
14	6	100	125	67.92	67.86
15	9	100	150	65.82	66.04
16	6	150	100	67.89	68.10
17	3	50	125	62.87	62.85

2.5 Adsorption Optimization Study

The copper stock solution, with a concentration of 1000 ppm and pH, is made by dissolving 2.81 g of CuSO_4 in 100ml of distilled water placed in a beaker. The solution was subsequently moved to a standardized volumetric flask and diluted with distilled water to reach a final volume of 1000ml. Experimental trials were carried out according to the details provided in Table 1. For each run, 40ml of the desired initial concentration and composite materials were mixed in a conical flask with a constant dosage of 1g, and the mixture was shaken at a specified shaken speed. After each experiment, the solutions were passed through a filter and analyzed with atomic absorption spectroscopy. Equation (1) below is used to calculate the percentage Cu^{2+} removed.

$$\text{Percentage Cu}^{2+} \text{ ion removal rate} = \frac{C_o - C_f}{C_o} \times 100 \quad (1)$$

Initial concentration of Cu^{2+} ions is represented by C_o (mg/L) and the final concentration of Cu^{2+} represented by C_f (mg/L).

2.6 Investigation of Adsorption Kinetics

Accurately assessing the interaction of copper (II) ions with coconut shell activated carbon required the use of adsorption isotherms. The experiment involved testing four distinct concentrations- 100, 150, 200 and 250 mg/L- under optimal conditions of pH 6, a shaking speed of 150rpm, and a constant adsorbent dosage of 1g. Measurements were taken at various time intervals: 15, 30, 90, 150, 210, 270, and 330 minutes for each concentration. The

quantity of Cu (II) adsorbed per unit mass of adsorbent, denoted as q_t (mg/g) was determined using Equation (2).

$$\text{Cu(II) concentration adsorbed at time } t; q_t = \frac{(C_o - C_t)}{W} V \quad (2)$$

Where C_o and C_t represent concentrations at the start and end (mg/L) correspondingly, here, W denotes the adsorbent mass. Likewise, Equation (3) was applied to calculate the equilibrium adsorption capacity, q_e which represents the quantity of Cu (II) removed from the solution.

$$\text{Cu (II) uptake at equilibrium, } q_e = \frac{(C_o - C_e)}{W} V \quad (3)$$

Where C_e indicates the concentration of the solution at equilibrium (mg/L).

Three different kinetic models were used to analyze the kinetic rates of the experimental data, including the Pseudo-first order model (Equation (4)), pseudo-second order (Equation (5)), and intraparticle diffusion models (Equation (6)).

$$\ln(q_t - q_e) = \ln(q_e - K_1 t) \quad (4)$$

$$\frac{t}{q_t} = \frac{1}{K_2 q_e} + \frac{t}{q_e} \quad (5)$$

$$q_t = K_3 t^{(1/2)} + C \quad (6)$$

where K_1 (min^{-1}) and K_2 (mg/g.min) represent the adsorption rate constants, while K_3 denotes the intraparticle diffusion constant.

2.7 Adsorption Equilibrium Isotherm

The adsorption equilibrium data from this study were analyzed using the isotherm models of Langmuir, Freundlich, and Temkin. As defined in Equation (7), the Langmuir isotherm model indicates that the adsorption takes place on a homogeneous surface with a monolayer of adsorbate (Garba *et al.*, 2016). The linear form of this model is represented in Equation (8).

$$q_e = \frac{q_m K_L C_e}{1 + K_L C_e} \quad (7)$$

$$\frac{C_e}{q_m} = \frac{C_e}{q_m} + \frac{1}{K_L q_m} \quad (8)$$

Where q_m represents the maximum adsorption capacity (mg/g) and K_L (L/mg) denotes the Langmuir constants related to the maximum adsorption capacity, respectively. Using Equation (8), a plot of C_e / q_e versus C_e yields a slope $1/q_m$ and intercept of $1/(K_L q_m)$. The Langmuir isotherm separation factor R_L , is denoted by Equation (9). R_L indicates the effectiveness of the adsorption process

$$R_L = \frac{1}{1 + K_L C_o} \quad (9)$$

K_L is the adsorption constant (L/mg) and C_o is the initial concentration of the adsorbate (mg/L). Moreover, the Freundlich adsorption isotherm model is represented by Equation (10) and linearizing the exponential result in Equation (11).

$$q_e = K_F C_e^{1/n} \quad (10)$$

$$\log q_e = \log K_F + \frac{1}{n} \log C_e \quad (11)$$

Here, K_F is the Freundlich constant (mg/g) (l/mg)^{1/n}, where 1/n represents the adsorption intensity which reflects the spread of adsorption energy and the variability in the surface characteristics.

The Temkin adsorption isotherm incorporates a factor that specifically addresses the interactions between the adsorbate and the adsorbent. According to the Temkin model as described in Equations (12) and (13), the heat of adsorption which depends on the temperature of the molecules within the layer, decreases linearly with increasing surface coverage (Ayawei *et al.*, 2017). It is important to note that the Temkin isotherm is not applicable across a broad range of ion concentrations.

$$q_e = \frac{RT}{b} \ln (A_T C_e) \quad (12)$$

$$q_e = B \ln A_T + B \ln C_e \quad (13)$$

Where $B = \frac{RT}{b}$ represents the constant associated with heat of adsorption (J/mol).

Here, A_T , b , R , and T refer to the Temkin isotherm equilibrium binding constant (L/mg), the Temkin isotherm constant, universal gas constant (8.314 J/mol. K), and the room temperature (298K), respectively. Thus, plotting q_e against C_e yields a gradient B and a constant term of $B \ln A_T$.

2.8 Study of Adsorption Thermodynamics

Temperature plays a significant role in determining both adsorption capacity and adsorption kinetics. Thermodynamics studies were conducted to investigate this effect by varying temperatures at 303, 313 and 323 K while maintaining at optimal pH of 6, a shaking speed of 150 rpm, and a consistent adsorbent dosage of 1 g. The experiment was performed with time intervals of 15, 30, and 90, 150, 210, 270 and 330 minutes, with an initial concentration consistently set at 150mg/L. Key thermodynamic parameters, including the changes in free energy (ΔG), enthalpy (ΔH), and entropy (ΔS) were analyzed. Equations (14) and (15) below were used for the calculations.

$$\ln (K_d) = \frac{\Delta G}{R} - \frac{\Delta G}{RT} \quad (14)$$

$$\Delta G = -RT \ln (K_d) \quad (15)$$

Where R is the universal gas constant (8.314 J/mole K), T is the temperature (K), and K_d is the distribution coefficient for adsorption.

3.0 RESULTS AND DISCUSSION

3.1 Adsorption Equilibrium Isotherm

Design-Expert 10.0.8.0 software (Stat-Ease, Inc; Minneapolis) was employed for experimental design and the subsequent analysis of variance (ANOVA). The statistical analysis for removal of heavy metal was done using analysis of variance (ANOVA). Multiple regression analysis was utilized to assess the impact of the independent variables (A-PH, B-Concentration (mg/l) and C- shaking speed (rpm) on the dependent variable (heavy metal removal). This gives a second-order polynomial equation, which was modified alongside with the significant model terms AB, AC and AB. The quadratic model obtained as shown in Equation (16) depicts the relationship between the removal of the dependent variable and the coded values of the independent variables A, B, and C, where Y represent the percentage heavy metal removal.

$$Y = 67.86 - 3.12A + 3.56B - 2.42C - 3.56A^2 - 0.38B^2 + 1.29C^2 - 0.63AB + 1.15AC + 1.82BC \quad (16)$$

Model's F-value of 409.77 as shown in Table 3, indicating the statistically significant of the model was obtained using the response surface model's Analysis of Variance. The obtained P-values less than 0.0001 also confirms the significance of all the model terms. Insignificant error in model fit value clearly shows how well the model fits the independent factors considered in this study. The coefficient of determination (R-Squared) and adjusted R-Squared (adj. R-Squared) are key metrics that reflect the effectiveness of the quadratic model. According to Figure 1a, the predicted R² of 0.9783 is in reasonable agreement with the adj. R² of 0.9957, with difference less than 0.2. The adj. R² value of 0.9957 is very close to 1, indicating an excellent fit. The values of the predicted R² and the adj. R² values are notably high and value close to 1 (or 100%) signifies a better fit. This demonstrates a strong relationship between the forecasted and observed Copper percentage removal. Given the model's statistical significance, it was utilized to determine the optimal conditions for achieving the highest removal of heavy metals. According to the proposed model, the ideal conditions for maximum heavy metal removal are pH 6, concentration (150 mg/L), and a shaking speed of 150 rpm, for 76.82% removal of Copper at a desirability of 1.000.

Figure 1(b-d) display a 3D landscape plot illustrating the interacting impact of the independent variables on removal efficiency of copper. Specifically, Figure 1b illustrates the influence of concentration and shaking speed. It was evident from the plot that the removal efficiency increases with increase in concentration and corresponding value of shaking speed. This depicts a mutual agreement between the concentration and the shaking speed as the increment of both factors result in high heavy metal removal efficiency. This result agrees with the ones obtained for the predicted and actual removal efficiency using both shaking speed and concentration as factors. Figure 1c also illustrate that removal efficiency increases with rising pH levels but decreases as concentration increases. Their cumulative impact happens to be one of the crucial parameters of the adsorption studies. Furthermore, in Figure 1d, it was observed that the removal efficiency was increasing with speed initially, until it gets to a point where the speed declines to 100 rpm and the pH was also observed to be declining. This in an indication that equilibrium is about to be reached.

Table 3: ANOVA Analysis for the Quadratic Response Surface Model

Source	Sum of Squares	Df	Mean Square	F-Value	P-Value	
Model	306.18	9	34.02	409.77	<0.0001	significant
A-pH	78.06	1	78.06	940.26	<0.0001	
B-Conc.	101.60	1	101.60	1223.80	<0.0001	
C-Speed	46.75	1	46.75	563.16	<0.0001	
AB	1.60	1	1.60	19.27	0.0032	
AC	5.29	1	5.29	63.72	<0.0001	
BC	13.32	1	13.32	160.47	<0.0001	
A²	53.30	1	53.30	641.94	<0.0001	
B²	0.60	1	0.60	7.24	0.0311	
C²	7.06	1	7.06	85.02	<0.0001	
Residual	0.58	7	0.083			
Lack of Fit	0.40	3	0.13	2.90	0.1649	Insignificant
Pure Error	0.18	4	0.046			
Cor Total	306.76	16				

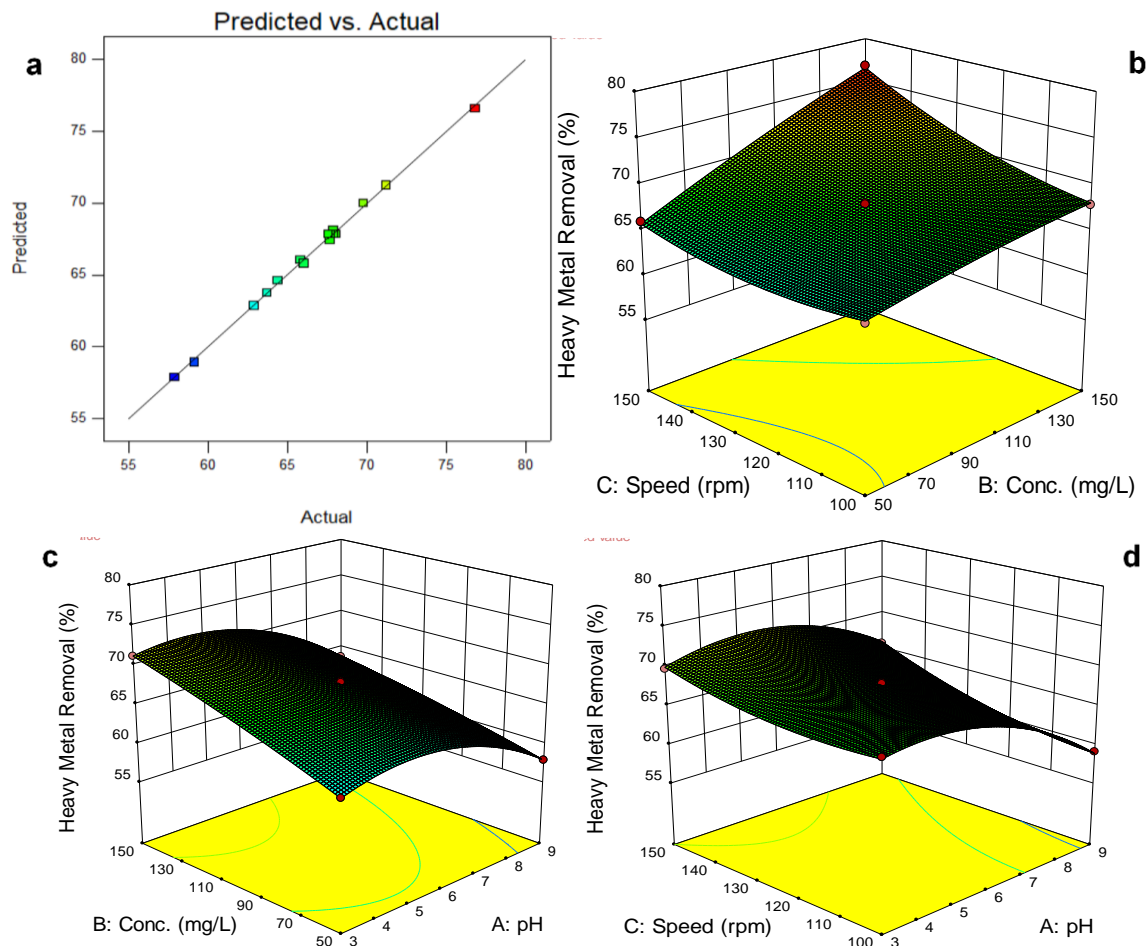


Figure 1: Efficiency of Cu^{2+} ions removal from synthetic wastewater (a), Interacting response between shaking speed and concentration (b), Interacting response between concentration and pH (c), Interacting response between shaking speed and pH (d).

3.2 Cu (II) Uptake Mechanism and Fourier Transform Infrared (FTIR) spectroscopy

The adsorption of Cu^{2+} ions involves the interactions between these ions and designated binding sites on the adsorbent material as illustrated in Figure 2. This process is primarily driven by complexation, ion exchange, and electrostatic attraction, which enable Cu (II) ions to bind to the adsorbent surface (Oribayo *et al.*, 2020). Complexation occurs when Cu (II) ions create stable coordination complexes with functional groups on the adsorbent. Electrostatic attraction plays a role in binding Cu(II) ions through interactions between positively charged metal ions and negatively charged sites on the adsorbent (Shah *et al.*, 2018). Several factors can affect the efficiency of Cu(II) uptake, such as pH, the presence of competing ions, and the specific characteristics of the adsorbent material. The pH of the CuSO_4 solution utilized in this work enhances the adsorption of Cu^{2+} ion. The functional groups on the chitosan-impregnated coconut shell adsorbent (CCSA) are impacted by this acidic environment and aid improves adsorption of copper ion on CCSA. This implies that electrostatic interactions between the positively charged Cu^{2+} ion and the negatively charged OH and $-\text{NH}_2$ functional group on CCSA are what propel adsorption. The diffusion and absorption of Cu^{2+} onto chitosan-impregnated coconut shell adsorbent composites are thus facilitated by this mechanism.

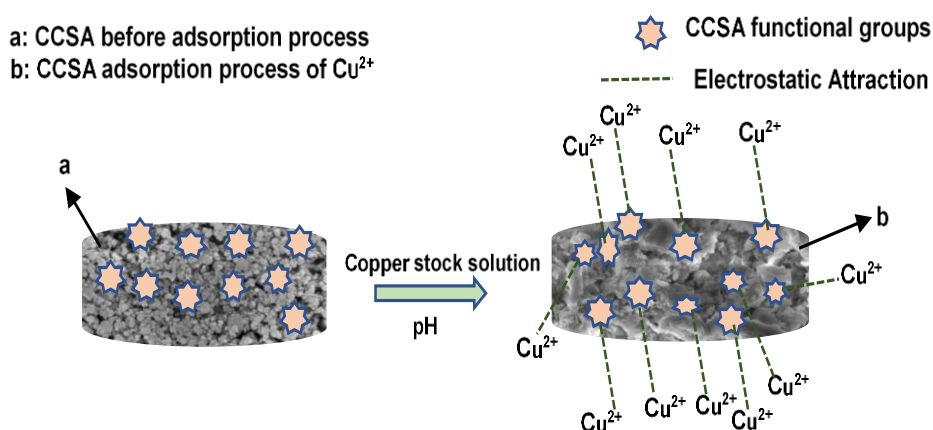


Figure 2: Schematic diagram for the adsorption of Cu^{2+} ion on chitosan-impregnated coconut shell Adsorbent.

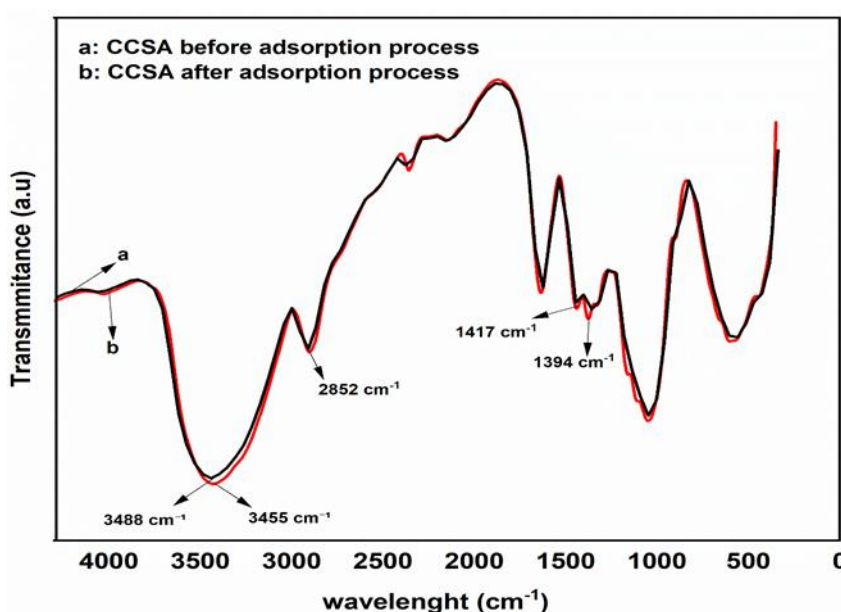


Figure 3: FTIR of chitosan-impregnated coconut shell adsorbent before and after adsorption process

The (FTIR) spectroscopy of the CCSA before and after adsorption as shown in Figure 3 is an essential tool for studying adsorption processes (Oribayo *et al.*, 2017). When molecules adhere to a surface, they cause alterations in the chemical environment of both the adsorbate and the adsorbent, which can be detected by FTIR, offering valuable information on the adsorption mechanism. The FTIR analysis of Samples of chitosan-impregnated coconut shell adsorbent (CCSA) before and after absorption, showed the existence of hydroxyl (OH), amine (-NH₂), and (-CH) stretching groups, with distinctive peaks reflecting chemical differences (Tegin *et al.*, 2023). The broad peak at 3488 cm⁻¹ and 3455 cm⁻¹ before and after the absorption of Cu²⁺ ions on CCSA indicate the presence of OH and -NH₂ functional groups. The slight shift in the peak wavelength before and after the adsorption is ascribed to the adsorption of Cu²⁺ onto OH and -NH₂ functional groups (Liu *et al.*, 2020). The ion-exchange process is the adsorption pathway for Cu²⁺ uptake, as evidenced by the FTIR spectra, which slightly shifts the wavelength of sorption peaks following adsorption. Additionally, the negatively charged ionizable functional groups -NH₂ and -OH on the CCSA surface have a strong ability to bind with the copper ion proton. The peak at 2852 cm⁻¹ is attributed to C-H stretching and the peaks at 1417 cm⁻¹, and 1394 cm⁻¹ are attributed to the C-H bending vibration (Ricciotti *et al.*, 2013).

3.3 Scanning Electron Microscopy (SEM) Analyses

SEM analysis is a powerful tool that enables the examination of material surfaces at extremely high magnifications. In this work, SEM was employed to evaluate and contrast the morphology of chitosan-impregnated coconut shell adsorbent composites before and after Cu²⁺ ions adsorption in synthetic wastewater. The SEM images of chitosan-impregnated coconut shell adsorbent before adsorption are depicted in Figure 4a and 4c, while Figures 4b and 4d show the chitosan-impregnated coconut shell adsorbent after adsorption. These detailed images provide insights into the surface morphology, allowing for a clearer identification of pore structures crucial to the adsorption process. From the morphology it could be observed that the pores of the chitosan-impregnated coconut shell adsorbent were not covered with the adsorbate, indicating the adsorbent have not undergo adsorption. On contrary, the pores of the chitosan-impregnated coconut shell adsorbent were covered with the adsorbate, indicating the adsorption process.

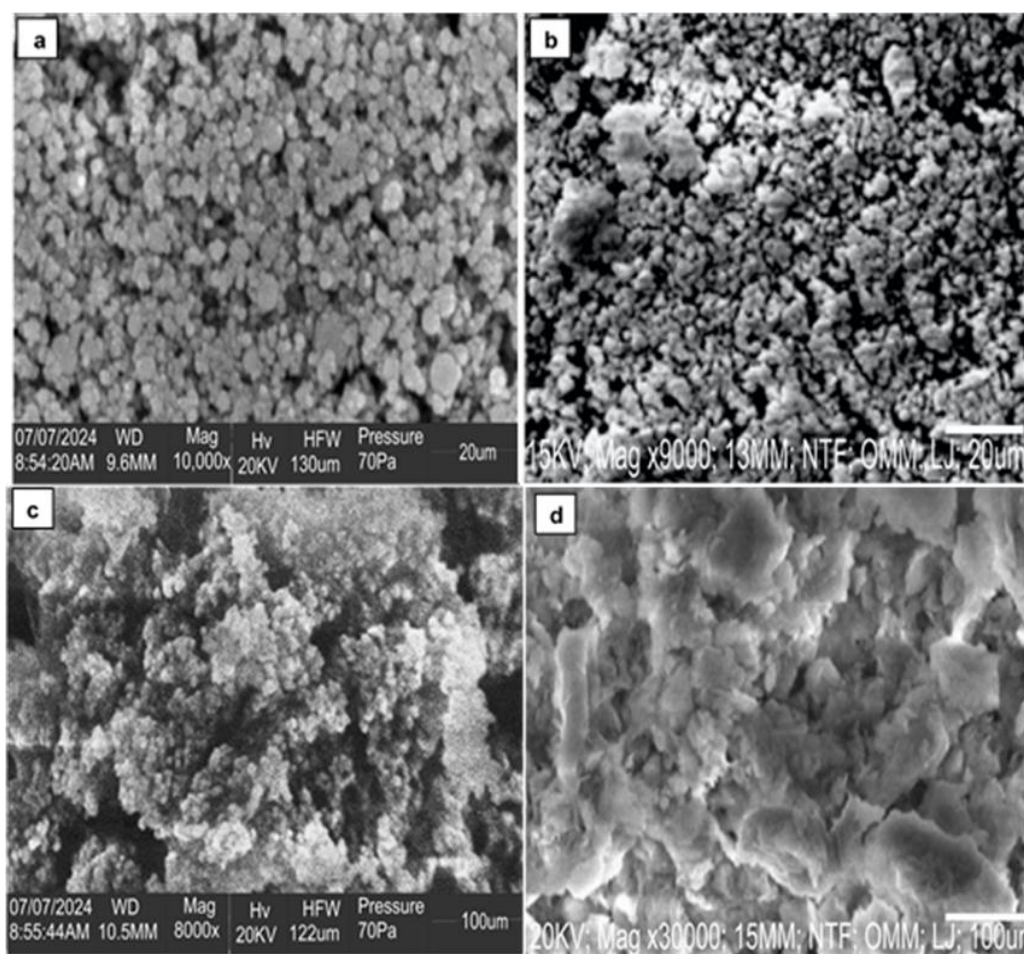


Figure 4: SEM images of chitosan-impregnated coconut shell adsorbent before adsorption (a, c) and after adsorption process (b, d)

3.4 Kinetics of Adsorption

The adsorption kinetics determines the rate-determining step, and the time required to complete the adsorption. Understanding how copper ions interact with the chitosan-impregnated coconut shell adsorbent is essential for evaluating the adsorbent's effectiveness and for designing and specifying adsorption columns. Therefore, adsorption kinetics models that account for the rate of copper ion uptake are critical for accurately designing copper effluent treatment processes. Figure 5a illustrates the impact of contact time on the adsorption capacity of chitosan-impregnated coconut shell adsorbent at varying copper ion concentrations. It was observed that the adsorption capacity for copper ions increased with contact time until equilibrium was reached at 330 minutes, achieving an adsorption capacity of 53.49mg/g for initial concentration of 150mg/L. The data indicates that swift rise in copper uptake can be attributed to a strong driving force, which enhances the rapid movement of copper ions to the CCSA composite. Contact time effect the uptake of copper ion was analyzed and compared against pseudo-first order, pseudo-second order, and intra-particle diffusion models, as illustrated in Figure 5b, 5c, and 5d, respectively. The findings, summarized in Table 4, revealed the R^2 values of these models across different copper ion concentrations. It was observed that R^2 values obtained from pseudo-first order and intra-particle diffusion models were less accurate compared to those from the pseudo-second order model. This suggests that the pseudo-second model provides a better fit for the kinetic experimental data and

pseudo-second order model aligns with findings from previous studies on copper adsorption from aqueous solutions.

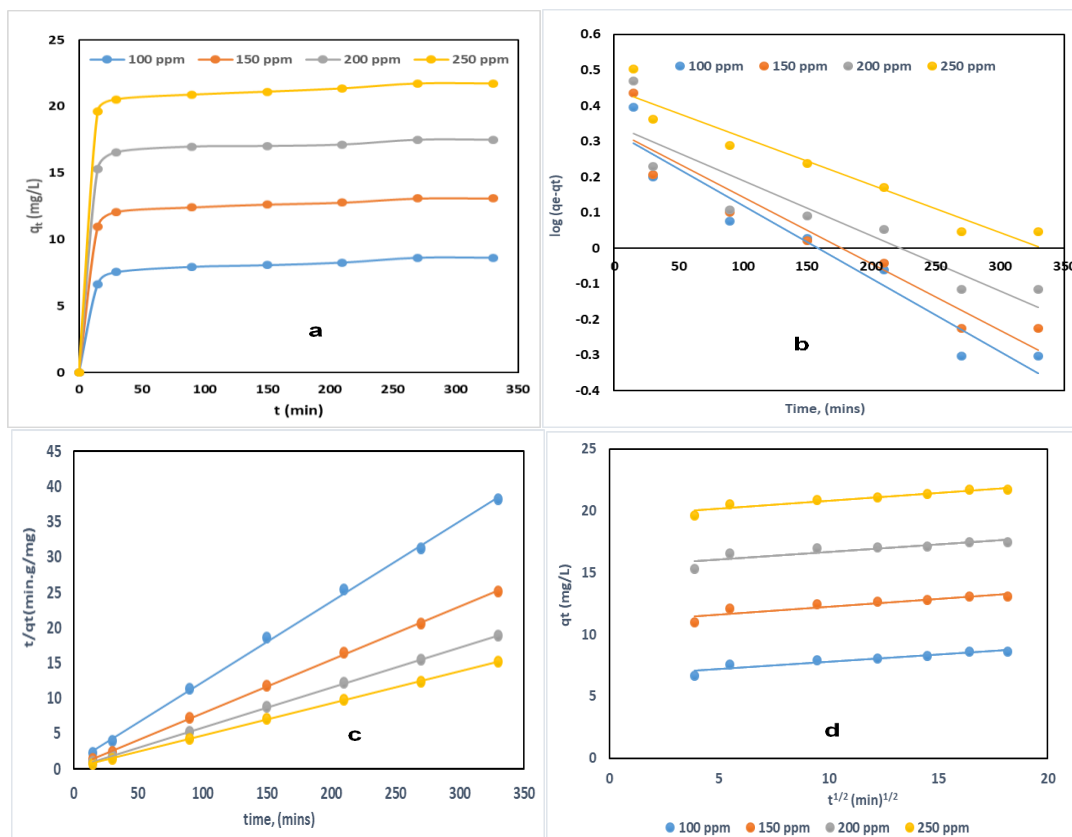


Figure 5: Effect of time on Cu (II) ions absorbed at different temperature (a), pseudo-first order kinetics for Cu (II) ions on chitosan-impregnated coconut shell adsorbent (b) pseudo- second order kinetic model for Cu (II) ions on chitosan-impregnated coconut shell adsorbent (c) intraparticle diffusion model for Cu (II) ion adsorption on chitosan-impregnated coconut shell adsorbent.

Table 4: Kinetic parameters for the adsorption of copper ions by chitosan-impregnated coconut Shell Adsorbent

Model	C ₀ (mg/ L)	q _e (mg/g)	q _{e cal} (mg/g)	K ₁ (min ⁻¹)	R ²	Δq(%)
Pseudo-first order	100	38.997	61.324	0.028	0.9271	57.253
	150	41.170	36.988	0.027	0.9003	10.16
	200	44.706	26.541	0.025	0.8307	40.63
	250	53.487	27.668	0.024	0.9252	48.27
Model Pseudo-second order	C ₀ (mg/ L)	q _e (mg/g)	q _{e cal} (mg/g)	K ₂ (gmg ⁻¹ min ⁻¹)	R ²	Δq(%)
	100	38.997	36.768	0.189	0.9989	5.71
	150	41.170	41.723	0.076	0.9997	1.32
	200	44.706	45.621	0.134	0.9998	2.04
Model Intra-Particle Diffusion	C ₀ (mg/ L)	q _e (mg/g)	C (mg/g)	K ₃ (mg/gmin ^{1/2})	R ²	Δq(%)
	100	38.997	33.045	1.017	0.8863	
	150	41.170	22.543	2.499	0.8408	
	200	44.706	23.657	5.423	0.7781	
250	53.482	20.614	7.143	0.9142		

3.5 Studies on Adsorption Isotherms

Adsorption equilibrium analyses establish a relationship between the adsorbate concentration in the solution and the amount of adsorbate captured onto an adsorbent at equilibrium stage. This process indicates how Cu (II) ions species are spread within solid and liquid adsorbent phases. It is expedient to determine the effectiveness of the adsorption study. To achieve this, copper (II) ions equilibrium data gotten from experiment are inserted into Langmuir, Freundlich, Temkin and Redlich-Peterson isotherms using equations 8, 10 11, 13. The R^2 correlation coefficient was the selection factor for inserting data obtained from experiment into the aforementioned isotherms.

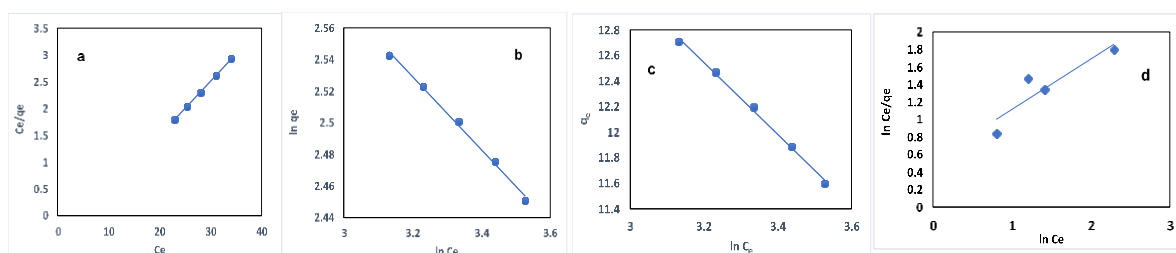


Figure 6 (a, b, c, d) represents Langmuir adsorption isotherm, Freundlich adsorption isotherm, Temkin adsorption isotherm and Redlich-Peterson adsorption isotherm of Cu (II) ions on chitosan-impregnated coconut shell adsorbent respectively.

As obtained in Figure 6a, 6b, 6c, and 6d, the R^2 values for Langmuir, Freundlich, Temkin and Redlich-Peterson were 0.9993, 0.9951, 0.9968 and 0.8251, accordingly. The results of the linear regression summarized in Table 5 show that Redlich-Peterson was not a good fit in comparison with Langmuir, Freundlich, and Temkin isotherms, which fit in perfectly. From the earlier stated linear regression results, the Langmuir isotherm is considered as the best coefficient of correlation. This implies the adsorption of copper ion on chitosan-impregnated coconut shell adsorbent composites is monolayer and homogenous at the interface, as well as no interaction between the copper ion species on the different site of the adsorbent interface. Thus, adsorption of Cu (II) ion unto chitosan-impregnated coconut shell adsorbent yields a positive result.

Table 5: Parameters for Copper Ion Adsorption unto Chitosan-impregnated Coconut Shell Adsorbent

Models	Isotherm constants				
Langmuir	Temperature (K)	Q_a (mg/g)	K_L (L/mg)	R_L	R^2
	298	201.23	0.04	0.20	0.9993
Freundlich	Temperature (K)	$1/n$	K_F (mg/g)(L/mg) ^{1/n}	N	R^2
	298	0.75	4.69	1.82	0.9951
Temkin	Temperature (K)	B	A_T (L/mg)	B	R^2
	298	33.41	0.32	96.17	0.9968
Redlich – Peterson	Temperature (K)	B	A (L/mg)		R^2
	298	0.45	5.02		0.8251

3.6 Studies on the Thermodynamics of Adsorption

Temperature effect on the uptake of copper unto chitosan-impregnated coconut shell adsorbent was examined to provide a more detailed understanding of the processes involved in adsorption. At an adsorbate concentration of 150 mg/l, temperatures of 303, 313 and 323K,

the thermodynamics studies were conducted. The enhancement in the adsorption capacity of the prepared CCSA composites was due to increase in pore dimensions, activation of surface functional groups and temperature (Sharma et al; 2010). As shown in Table 6, ΔS , ΔH and ΔG for Cu^{2+} ions adsorption on chitosan-impregnated coconut shell adsorbent composite were determined using thermodynamic equations 14 and 15. ΔH and ΔS values were obtained from the gradient and intercept, respectively, by plotting $\ln K_d$ against $1/T$ illustrated in Figure 7. The positive value of ΔH (2859.3 J/mol), indicate copper (II) ion adsorption on the chitosan-impregnated coconut shell adsorbent is an endothermic reaction. In addition, the positive value of ΔS , indicates the attraction of the adsorbate unto the chitosan-impregnated coconut shell adsorbent composite and its electrostatic attraction driven mechanism. The $-\Delta G$ values show spontaneity as well as thermodynamics practicability.

Table 6: Copper (II) ions Thermodynamics Adsorption Parameters

$\Delta H(\text{J/mole})$	$\Delta S(\text{J/mole}) (\text{K})$	$-\Delta G(\text{J/mole})$		
		303K	313K	323K
2859.3	10.715	632.855	1167.041	1681.427

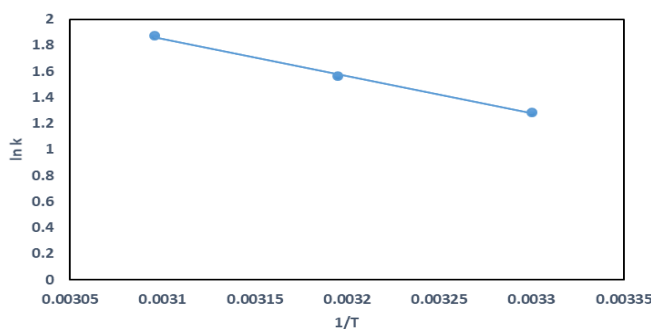


Figure 7: Graph of $\ln (K_d)$ versus $1/T$ for the adsorption of copper (II) ion onto chitosan-impregnated Coconut shell adsorbent composites

3.7 Contrast between Adsorption Capacity for Cu^{2+} ions Removal

This study’s primary focus is to create effective, low-cost adsorbents for treating water contaminated with copper. Recent research has concentrated on utilizing various inexpensive materials for copper removal from wastewater. The composite of chitosan-impregnated coconut shell adsorbent (CCSA) synthesis in this study compares favorably with existing reported adsorbent in literature as shown in Table 7. Notably, CCSA adsorbent exhibits a higher adsorption capacity compared to some adsorbents, such as calcium carbide waste, sugarcane bagasse, waste pineapple peel biomass and maize cob. Additionally, the chitosan-impregnated coconut shell adsorbent is an affordable option since it is derived from agricultural waste that otherwise contributes to environmental pollution. Its cost-effectiveness makes it a more favorable choice compared to the aforementioned adsorbents.

Table 7: Adsorbent Comparison for Copper Removal

Adsorbents	Adsorption Capacity (mg/g)	References
Grape bagasse	43.47	Demira, et al. (2016)
zeolitic materials	93.72	Shah et al. (2013)
Biogenic Iron precipitate	7.54	Oladipo et al. (2021)
Waste corn cob	53.36	Saadi et al. (2024)
Tunisian date stones	31.25	Bouhamed et al. (2012)

Banana leave activated carbon	66.2	Darweesh, et al. (2022)
CCSA	53.49	This work

4. CONCLUSION

In this investigation, chitosan-impregnated coconut shell adsorbent (CCSA) composite was produced from chitosan and coconut shell and utilized to investigate the adsorption of copper in synthetic wastewater. The efficiency of copper removal by the prepared CCSA adsorbent was optimized using RSM. A 76.82% removal rate of Cu^{2+} ion was achieved at an optimal pH of 6, initial concentration of 150 mg/L. The equilibrium adsorption data for Cu^{2+} ions on the CCSA composite fit the Langmuir isotherm model. Furthermore, Pseudo-second order explicitly aligned with the kinetic data. Thermodynamic analysis, including parameters ΔH , ΔS , and ΔG , revealed that the adsorption process of Cu^{2+} ions onto the CCSA composite is endothermic and spontaneous. These outcomes indicate that the prepared chitosan-impregnated coconut shell adsorbent, offering a practical solution for wastewater treatment.

REFERENCES

- Abdel-Ghani, N.T., El-Chaghaby, G.A. (2014). Biosorption for metal ions removal from aqueous solutions: a review of recent studies. *Int. J. Latest Res. Sci. Technol.* 3 (1), 24–42.
- Acharya, J., Sahu, J. N., Mohanty, C. R., & Meikap, B. C. (2009). Removal of lead (II) from wastewater by activated carbon developed from Tamarind wood by zinc chloride activation. *Chemical Engineering Journal*, 149(1-3), 249-262. <https://doi.org/10.1016/j.cej.2008.10.029>
- Bouhamed, F., Elouear, Z., & Bouzid, J. (2012). Adsorptive removal of copper (II) from aqueous solutions on activated carbon prepared from Tunisian date stones: Equilibrium, kinetics, and thermodynamics. *Journal of the Taiwan Institute of Chemical Engineers* 43, 741–749.
- Darweesh, M.A., Elgendy, M.Y., Ayad, M.I., Ahmed, A.M., Elsayed, N. M. K., & Hammad, W.A. (2022). Adsorption isotherm, kinetic, and optimization studies for copper (II) removal from aqueous solutions by banana leaves and derived activated carbon. *South African Journal of Chemical Engineering*, 40, 10-20. <https://doi.org/10.1016/j.sajce.2022.01.002>
- Demiral, H., & Gungor, C. (2016). Adsorption of copper (II) from aqueous solutions on activated carbon prepared from grape bagasse. *Journal of Cleaner Production*. 124 (15), 103-113. <https://doi.org/10.1016/j.jclepro.2016.02.084>
- Ganji, H., & Taghavijeloudar, M. (2024). Efficient adsorption of lead and copper from water by modification of sand filter with a green plant-based adsorbent: Adsorption kinetics and regeneration. *Environmental Research*. 259, 15, 119529. <https://doi.org/10.1016/j.envres.2024.119529>
- Hafez, O. A., Mohamed, R. R., Kana, T. H. A., Mohamed, E. A., & Negm, N. A. (2022). Treatment of industrial wastewater containing copper and lead ions using new carboxymethyl chitosan-activated carbon derivatives. *Egypt. J. Chem.* 65 (2), 123 - 132. <https://doi.org/10.21608/ejchem.2021.82163.4050>
- Liu, J., Yang, X., Liu, H., Cheng, W., & Bao, Y. (2020) Modification of calcium-rich biochar by loading Si/Mn binary oxide after NaOH activation and its adsorption mechanisms for removal of Cu (II) from aqueous solution. *Colloids Surf A Physicochem Eng Asp.* 601, 124960. <https://doi.org/10.1016/j.colsurfa.2020.124960>
- Myers, R. H., Montgomery, D. C., & Anderson-Cook, C. M. (2016). *Response surface methodology: Process and product optimization using designed experiments* (4th Ed.)
- Oladipo, B., Govender-Opitz, E., & Ojumu, T. V. (2021). Kinetics, Thermodynamics, and Mechanism of Cu (II) Ion Sorption by Biogenic Iron Precipitate: Using the Lens of Wastewater Treatment to Diagnose a Typical Biohydrometallurgical Problem. *ACS Omega*. 6 (42). 27984–27993. <https://doi.org/10.1021/acsomega.1c03855>
- Oribayo, O., Olalekan, A. P., Owolabi, R. U., Olaleye, O. O., & Onyekaba, O. A., (2020). Adsorption of Cr (VI) ions from aqueous solution using rice husk-based activated carbon: optimization, kinetic, and thermodynamic studies. *Environ Qual Manage.* 1–17. <https://doi.org/10.1002/tqem.21704>

- Oribayo, O., Feng, X., Rempel, G. L., & Pan, Q. (2017). Synthesis of Lignin-based polyurethane/graphene oxide foam and its application as an absorbent for oil spill clean-ups and recovery. *Chem Eng J.* 323, 191–202. <https://doi.org/10.1016/j.cej.2017.04.054>
- Ricciotti, L., Roviello, G., Tarallo, O., Borbone, F., Ferone, C., Colangelo, F., Catauro, M., & Cioffi, R. (2013). Synthesis and characterizations of melamine-based epoxy resins. *Int.J.Mol.Sci.*, 14, 18200 -18214. <https://doi.org/10.3390/ijms140918200>
- Saadi. B. M., Naeem, Y. A., Alhameedi, D.Y., Hussein, T. K., Idan, A. H., & Dawood, I. I. (2024). Conversion of Waste Corn Cob to Highly Green Surface Activated Carbon: Removal and Adsorptive of Copper Ions from Aqueous Solution. *Asian Journal of Green Chemistry*, 8(6), 710-721. <https://doi.org/10.48309/AJGC.2024.473357.1544>
- Seleman, M., Sime, T., Ayele, B., Sergawie, A., Nkambule, T., & Fito, J. (2023). Isotherms and Kinetic Studies of Copper Removal from Textile Wastewater and Aqueous Solution Using Powdered Banana Peel Waste as an Adsorbent in Batch Adsorption Systems. *International Journal of Biomaterials*. 1-10. <https://doi.org/10.1155/2023/2012069>
- Shah, B. A., Mistry, C. B., & Shah, A.V. (2013). Sequestration of Cu (II) and Ni (II) from wastewater by synthesized zeolitic materials: Equilibrium, kinetics and column dynamics. *Chemical Engineering Journal*. 220, 172-184. <https://doi.org/10.1016/j.cej.2013.01.056>
- Tegin, I, Oc, S., Saka, C. (2023). Adsorption of copper (II) from aqueous solutions using adsorbent obtained with sodium hydroxide activation of biochar prepared by microwave pyrolysis. *Biomass Conversion and Biorefinery*. <https://doi.org/10.1007/s13399-024-05477-6>
- Vaiopoulou, E., & Gikas, P. (2012), Effects of chromium on activated sludge and the performance of wastewater treatment plants: A review, *Water Res.* 46, 549-570. <https://doi.org/10.1016/j.watres.2011.11.024>
- Wang, J., & Chen, C. (2009). Biosorbents for heavy metal removal and their future. *Biotechnology Advances*, 27(2), 195-226. <https://doi.org/10.1016/j.biotechadv.2008.11.002>
- Xue, J, Cui Q, Bai Y., Wu Y., Gao Y., Li L., & Qiao, N. (2016). Optimization of adsorption conditions for the removal of petroleum compounds from marine environment using modified activated carbon fiber by response surface methodology. *Environ Prog Sustain Energy*. 35(5), 1400-1406.